

Dynamic Economic Dispatch using Complementary Quadratic Programming

Dustin McLarty, Nadia Panossian, Faryar Jabbari, and Alberto Traverso

Abstract -- Economic dispatch for micro-grids and district energy systems presents a highly constrained non-linear, mixed-integer optimization problem that scales exponentially with the number of systems. Energy storage technologies compound the mixed-integer or unit-commitment problem by necessitating simultaneous optimization over the applicable time horizon of the energy storage. The dispatch problem must be solved repeatedly and reliably to effectively minimize costs in real-world operation. This paper outlines a methodology that greatly reduces, and under some conditions eliminates, the mixed-integer aspect of the problem using complementary convex quadratic optimizations. The generalized method applies to grid-connected or islanded district energy systems comprised of any variety of electric or combined heat and power generators, electric chillers, heaters, and all varieties of energy storage systems. It incorporates constraints for generator operating bounds, ramping limitations, and energy storage inefficiencies. An open-source platform, EAGERS, implements and investigates this optimization method. Results demonstrate the efficacy of the optimization method benchmarked against a commercial mixed-integer solver.

Index Terms-- Economic dispatch, energy storage, quadratic programming, unit commitment, mixed-integer relaxation

I. INTRODUCTION

TECHNOLOGY advances, environmental policy, and energy market de-regulation have spurred deployment of distributed generators, small renewable installations, and large energy storage systems. Traditional paradigms relying on centralized power generation distributed through medium and low voltage networks, are adapting to incorporate aggregated systems of distributed generators (i.e., microgrids). To the individual user, microgrids provide the same power as the grid with the potential to improve reliability, power quality, and environmental impact through controls and co-production of heating and cooling [1]. The complexity of a combined cooling heating and power (CCHP) microgrid stems from the coupled interaction between electricity, heat and cooling production, the competing objectives (cost, efficiency, emissions and reliability), and disparate time-scales of response [2]. Stochastic loads, such

as electric vehicle charging, intermittent renewable power generation, energy storage, and participation in ancillary grid service markets further complicate the energy management problem.

Energy storage, in particular, offers tremendous potential to improve energy management in district energy systems. Energy storage systems are designed and utilized for one or more purposes; load smoothing, peak shaving, and energy arbitrage. Small capacity energy storage, storing less than 1% of daily use, is typically applied to ‘load smoothing’: balancing short-term disparities between demand and generation arising due to limitations in generator responsiveness. Intermediate scale energy storage, storing less than 5% of daily use, often provides ‘peak shaving’: avoiding short term power surges which incur peak demand tariffs (\$/kW) by augmenting generation during peak load events. Larger storage systems, storing more than 5% of daily use, provides arbitrage, i.e. shifting consumption from expensive periods to inexpensive periods. Management to accomplish all three is a challenging control problem closely tied to the scheduling of all other distributed energy assets. Management techniques must repeatedly and reliably dispatch all systems in a timely fashion in order to minimize operating costs and maximize the utility of storage assets.

Economic dispatch is a centralized approach to determining the optimal scheduling of generators, known as unit commitment. This paper focuses on efficiently and reliably solving the centralized economic dispatch problem, but should be seen as complementary to other methods of microgrid dispatch. Multi-agent control is a promising decentralized control method [3,4,5] with advantages when developing ‘plug-and-play’ generators. With a pre-defined communication system, generators can be readily integrated into a bidding process which allocates generation duties between network systems using market based strategies. The drawback to decentralized control is the loss of capability that forecasting provides, which becomes paramount in the presence of energy storage. Centralized control has the potential to see the bigger picture and dispatch generators according to present demands, while anticipating future demands. However, the informational requirements of centralized control can be substantial [6]. The information requirements include the costs, capacity, performance and response capabilities of each distributed energy resource (DER), the time-of-day and/or weather dependence of the load, and the grid costs and interconnection constraints. Centralized controllers may also include market type bidding strategies when selling capacity or ancillary services to the grid [1,7].

Methods for determining economic dispatch include a number of heuristic [8] or metaheuristic search methods including genetic algorithms [9,10], mixed integer linear programming [10], dynamic programming [11], and simulated annealing methods [12]. Search methods have been inspired by metal processing (i.e. simulated annealing)

[13,14], or a biology (e.g. Particle Swarm, Artificial Immune System, Ant Colony, Bacterial Foraging, Firefly) [15-22].

The majority of these methods are applied to electrical demands only [1,3,4,6,9,15,19]. Some are able to balance multiple objectives such as cost and emissions [16,23], or electrical and heating demands [17,20,22]. Forecasting uncertainty, specifically wind generation, can be addressed with neural network or particle swarm approaches [15]. Generator constraints such as operating limits, response rates, and re-start costs are difficult to consider without solving a mixed integer problem [24], and are often disregarded [1].

As distributed resources, energy storage, and renewable power systems become more prevalent, new methods of scheduling and dispatching systems are necessary. Fast, Reliable and repeatable optimal scheduling can simultaneously reduce costs, reduce emissions, and improve reliability of our energy delivery. This paper introduces a methodology, which addresses the limitations of current economic dispatch optimization techniques. The methodology utilizes quadratic programming to simultaneously consider the dispatch over a finite forecast horizon and capture the non-linear performance and cost of generators with less computational demand than typical mixed-integer unit commitment techniques.

II. METHODOLOGY

The following methodology describes a modified dynamic economic dispatch formulation for solving the economic dispatch of systems with energy storage, particularly co-located distributed energy or microgrid scale systems. Generally, unit commitment/economic dispatch is a mixed-integer problem with $2^{N \cdot G}$ binary decision variables determining the on/off status and output each of the G generators at each time step from 1 to N . The order of the mixed-integer problem quickly increases beyond what is practical to solve. For example, a system with just 4 dispatchable generators would have 16 possible operating configurations at any time. Adding energy storage and solving for the optimal dispatch at each hour of a day results in 2^{96} or 7.92×10^{28} total configurations.

Three solution methods are presented to solve the same convex problem formulation:

- i. FMI, full mixed-integer solution
- ii. cQP, complementary quadratic programming
- iii. mcQP, modified complementary quadratic programming

The quadratic programming methods, proposed herein, utilize an open-source interior-point algorithm. The full-

mixed integer (FMI) method uses a commercial software package, Gurobi®, to solve the convex optimization with $2^{N \cdot G}$ binary decision variables. The cQP method solves two convex optimizations with no binary decision variables. The cQP method determines the on/off status of each system after the first optimization, with some potential loss in optimality. The modified method, mcQP, regains some optimality by solving N mixed-integer sub-problems each with only 2^G binary decision variables. Both cQP and mcQP methods reliably and repeatedly solve the dispatch problem faster than FMI, which can often fail to find a feasible solution for complex problems.

The reduced computational burden makes the quadratic programming methods applicable to a receding horizon control approach. The methods are implemented within an open-source platform for the design, simulation, and control of district energy systems. The Efficient Allocation of Grid Energy Resources including Storage (EAGERS) tool and source code can be accessed at <https://github.com/CESI-Lab/EAGERS> or by contacting the corresponding author.

Formulating the optimization problem

Equation (1) identifies the objective function used to minimize energy costs by determining the optimal generator power output, P_i , grid power, P_{grid} , and energy storage state-of-charge, SOC_r , at each time step, k . There are N time steps, $k = 1, 2, 3, \dots$, and G dispatchable generators whose cost, $F(P_i)$, is a convex function of their power output. A time dependent price for either purchasing or selling power, $F(P_{grid})$, represents an interconnection agreement with an external electric grid. Valuing energy that remains stored in the S energy storage devices at the end of the forecast horizon, $\{F(SOC_r)\}_N$, ensures that solutions which fully deplete the storage are not always preferred.

$$\min C = \sum_{k=1}^N \left\{ \sum_{i=1}^G F(P_i)_k + F(P_{grid})_k \right\} + \sum_r^S \{F(SOC_r)\}_N \quad (1)$$

The ‘cost’ of energy storage devices accrues when additional generation is required to charge the storage. By not applying costs to the state-of-charge, SOC_r , at intermediate time steps, the storage can be dispatched to provide the greatest value when discharging and charge when the marginal cost of energy is lowest. This approach differs from many common unit-commitment solutions that assign a cost to energy drawn from storage that represents the average cost of energy generation plus some factor which accounts for the round-trip inefficiencies. The formulation is further described in appendix I.

The minimization of (1) is constrained at every time step, $k = 1, 2, 3 \dots N$, by an energy balance equality (2). The energy demand categories, e.g. AC power, DC power, heating, cooling, or steam production, each have a separate energy balance constraint.

$$\forall k \quad \sum_{i=1}^G (P_i)_k + (P_{grid})_k + \sum_{r=1}^S (P_r - \phi_r)_k - (P_{loss})_k = L_k \quad (2)$$

Some generators or other devices appear in multiple energy balances, such as an electric chiller appearing in the cooling energy balance as a generator, P_i , and in the electric energy balance as a load, $-P_i\beta$, where β represents the conversion efficiency of the chiller. A loss term, P_{loss} , accounts for cases in which energy dissipation is possible, such as dissipation of excess heat produced by a boiler or combined heat and power device. An inequality constraint ensures $P_{loss} \geq 0$ so that no free energy is provided. The load, L , represents the forecasted demand which must be satisfied at each time interval.

Each generator is subject to its own ramping and capacity constraints, equations (3) and (4). When $P_i^{min} > 0$ the complexity of mixed-integer dispatch problem increases due to the discontinuity between off, zero or idling, and on. When $r_i^{max} \cdot \Delta t < (P_i^{max} - P_i^{min})$, the entire operating range is not available between successive time-intervals. This constraint applies to slow responding systems, such as high temperature fuel cells, or when the time intervals are short.

$$|(P_i)_k - (P_i)_{k-1}| \leq r_i^{max} \cdot \Delta t \quad (3)$$

$$P_i^{min} \leq P_i \leq P_i^{max} \quad (4)$$

Each storage device adds two terms to the energy balance constraint, P_r and ϕ_r . The useful power supplied to or extracted from the energy storage device, P_r , is related to the change in stored energy by equation (5). The second term in equation (6) accounts for the additional energy put into charging the storage device that cannot be recovered during discharge. Equation (6) relates the charging penalty to the changing state-of-charge. Both inequalities of (6) are enforced at each step. When charging, i.e. when $(SOC_r)_k > (SOC_r)_{k-1}$, the right hand side of the first inequality is greater than zero and the non-recoverable energy must be supplied by the generation. When discharging, the second inequality ensures that this non-recoverable energy is not recovered, i.e. $\phi_r = 0$. The energy storage charging and discharging efficiencies, represented by η_c and η_d , are constant.

$$(P_r)_k = - \frac{\{(SOC_r)_k - (SOC_r)_{k-1}\} \cdot \eta_d}{\Delta t_k} \quad (5)$$

$$(\phi_r)_k \geq \frac{\{(SOC_r)_k - (SOC_r)_{k-1}\}}{\Delta t_k} \cdot \left(\frac{1}{\eta_c} - \eta_d \right) \quad \& \quad (\phi_r)_k \geq 0 \quad (6)$$

The capacity constraint (7) and the charging/discharging constraint (8) further constrain the storage system.

$$SOC_r^{min} \leq SOC_r \leq SOC_r^{max} \quad (7)$$

$$P_r^{min} \leq P_r \leq P_r^{max} \quad (8)$$

Most storage devices are unable to store energy indefinitely. Equation (9) expands equation (5) to include self-discharge that is constant, κ , or proportional to the state of charge, κ^* . The value κ represents a constant discharge rate, e.g. 1kWh per hour or 1kW. The value κ^* represents the fraction of storage lost per hour from full charge. For example if a fully charged battery would lose 20% charge in the first hour $\kappa^* = 0.2$

$$(P_r)_k = - \frac{\{(SOC_r)_k - (1 - \kappa^* \cdot \Delta t_k) \cdot (SOC_r)_{k-1} - \kappa\} \cdot \eta_d}{\Delta t_k} \quad (9)$$

Because of uncertainty in forecasting loads, a receding horizon control method can fail when the dispatch solution fully charges or completely discharges the energy storage. Appendix II outlines a method that facilitates receding horizon control while maintaining the full capacity of the energy storage during dispatching.

Formulating the cost functions

The cost function of each generator, $F(P_i)$, can take a number of forms depending upon the solution methodology selected. Generally, the cost functions for most systems, e.g. generators, chillers, and cooling towers are non-linear and possibly non-convex. Non-convex cost functions imply multiple local minima, which introduces instability in a receding horizon control problem if the solution oscillates between local minima.

The input-to-output conversion efficiency (η) may be a non-linear function of output, depicted in Figure 1A. The standard unit commitment problem inverts efficiency to find the specific cost of generation (\$/kWh). Operators then bid their capacity as a unit at the lowest specific cost. Micro-grids cannot rely on nearly continuous curve of unit commitments due to the relatively small number of generating systems at their disposal. Considering the inefficiencies at part-load requires multiplying the cost of energy, (\$/kWh), by the energy delivered, kWh, which results in the non-linear operating cost (\$/hr), shown in Fig. 1A.

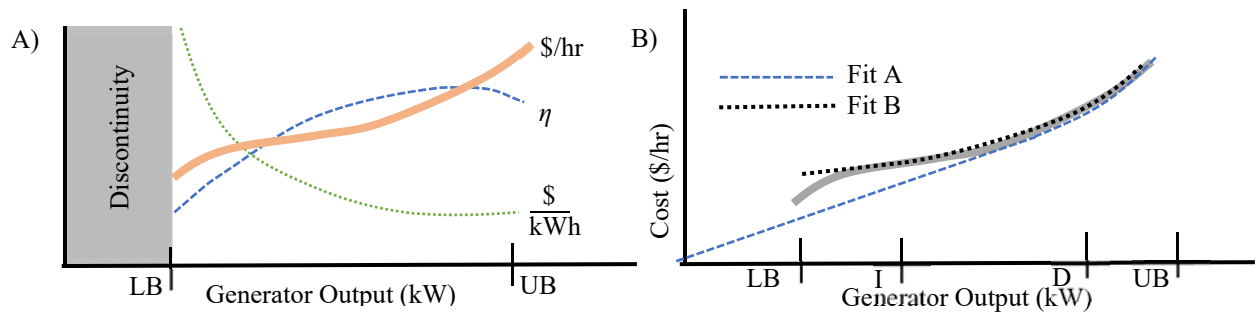


Figure 1 Conceptual depiction of generator performance and cost functions.

A) Typical electric generator efficiency (η), specific cost of generation (\$/kWh), and non-linear operating cost curve (\$/hr).

B) Piecewise convex quadratic cost functions. Fit A is linear from 0 to peak efficiency, D, and quadratic from D to the upper bound, UB. Fit B is discontinuous from 0 to the lower bound, LB, linear from LB to the cost curve inflection point, I, and quadratic from I to UB.

The approach taken solves a least-squares problem, detailed in appendix III, to fit two different convex piecewise quadratic polynomials to a set of measured data. **Fit A** represents the best possible piecewise convex quadratic that avoids the lower bound discontinuity and has zero cost at zero output. **Fit B** includes the discontinuity and has a non-zero initial cost. **Fit A** will typically have greater error in the low power output region, and closely approximate **Fit B** near nominal power. Appendix IV outline piecewise linear functions that represent the heat recovery of CHP devices, and the energy conversion efficiency of electric and absorption chillers.

The piecewise quadratic functions outlined in appendix IV are well suited for interior-point search methods. This study divided the operating region into five equal segments and determined the linear coefficients a_1, \dots, a_5 and the quadratic coefficients, b_1, \dots, b_5 detailed in Table 1. It is common practice in optimization approaches to estimate convex functions with a series of linear segments. However, when using an interior point method it is generally faster and more accurate to use a few quadratic segments than a multitude of linear segments. The quadratic costs have the benefit of smoother transitions in the solution, i.e. balancing the marginal cost of each generator within segments rather than at the segment endpoints.

Solving the optimization problem with cQP

This paper introduces the complementary Quadratic Programming method, cQP, to quickly and consistently solve the economic dispatch optimization with energy storage. The four step process outlined in Figure 2 begins with solving the problem formulation using **Fit A** coefficients and a relaxed constraint (4) that sets each generators lower constraint limit, P_i^{min} , to zero. This initial optimization results in a close approximation of the true optimal operation, but may be infeasible if one or more generators' scheduled output is within the relaxed constraint region between zero and P_i^{min} .

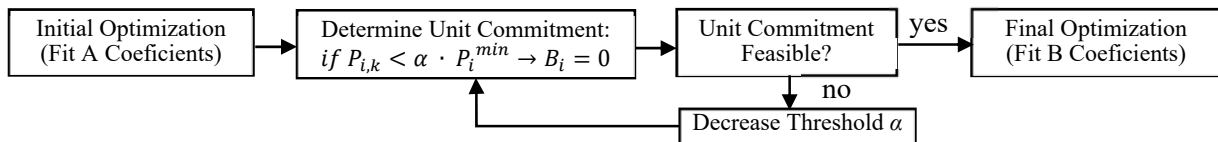


Figure 2 Process description of complementary Quadratic Programming

The cQP unit commitment first assumes all generators dispatched $< P_i^{min}$ are off, and thus set to zero output for the second and final optimization. Other systems must then pick up the slack. For the majority of cases this assumption results in a unit commitment that closely replicates that of an optimal solution. A second optimization utilizing this unit commitment and the coefficients of **Fit B**, determines the optimal dispatch solution, and enforces the original P_i^{min} constraint.

If the initial unit commitment is infeasible, then some generator initially assumed offline must be on with an output greater than P_i^{min} . Some of this production will meet demands while the remainder will be captured by energy storage or offset by other systems operating at reduced output. The cQP method finds a feasible unit commitment by lowering the threshold for determining on/off status to $\alpha \cdot P_i^{min}$, where $\alpha < 1$. Thus the generators closest to the operating threshold are added to the unit commitment schedule, and set to produce greater than their minimum output, P_i^{min} . The threshold is lowered until the unit commitment allows for a feasible optimization of the system. The vast majority of initial optimizations determine a feasible schedule without lowering the unit commitment threshold. For all district energy systems with sufficient capacity to meet demands, the cQP approach will find a feasible energy dispatch.

Solving the optimization problem with mcQP

For complex highly constrained district energy systems, or if system start-up costs are significant, it is beneficial to check a broader set of feasible operating conditions between the two complementary optimizations. The results will show that although cQP is fast, repeatable and reliable for a solution, its solution is typically less optimal than the FMI approach. A modified cQP approach, described in Figure 3, retains the repeatability and reliability of cQP, but regains some of the optimality of FMI. The mcQP approach solves the same initial and final optimizations, but spends more effort determining the unit commitment. After the initial optimization, mcQP consecutively solves N reduced mixed-integer sub-problems, each with only 2^G binary decision variables. A heuristic filter then accounts for start-up costs.

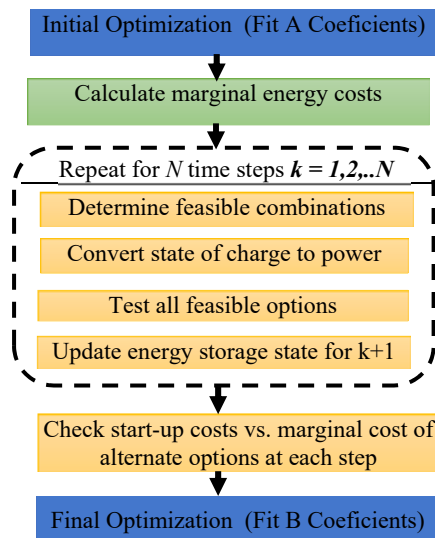


Figure 3 Process description for modified complementary Quadratic Programming

When optimizing a single time step, energy storage lacks the ‘big-picture’ perspective of the simultaneous

optimization. A modified formulation of the energy storage constraints, equations 5-9, outlined in Appendix V incorporates a multi-step perspective from the first optimization to determine the relative cost for each feasible subset of generators to meet the demand at each step. A boundary constraint ensures the sub-problem solutions do not excessively deviate from the energy storage profile of the initial optimization.

Equation (10) determines the feasibility of the 2^G possible combinations at each step. The binary variable $B_{i,k}$ is true when the generator is included in the subset.

$$\sum_{i=1}^G \{P_i^{min} \cdot B_{i,k}\} + P_{grid}^{min} + \sum_r^S P_r^{min} \leq L_k - P_{unctrl_k} \leq \sum_{i=1}^G \{P_i^{max} \cdot B_{i,k}\} + P_{grid}^{max} + \sum_r^S P_r^{max} \quad (10)$$

Equation (11) outlines the cost function for optimizing the energy dispatch at a single time step, k . The binary term, $B_{i,k}$, modifies the generator output constraint as shown in equation (12). The energy balance constraints, (2), can also include the constant term, β_0 , from **Fit B** multiplied by the binary status. The feasible combination of generators with the lowest relative cost at each step form an initial set of binary values.

$$Cost = \sum_{i=1}^G a_{0,i} \cdot B_{i,k} + \min \left\{ \sum_{i=1}^G F(P_i) + F(P_{grid}) + \sum_{r=1}^S F(P_r) \right\} \quad (11)$$

$$B_{i,k} \cdot P_i^{min} \leq P_{i,k} \leq B_{i,k} \cdot P_i^{max} \quad (12)$$

Start-up costs incurred each time a generator starts, c_i , can include the additional fuel use during warm-up or maintenance costs that are tied to the number of shutdowns or startups. Equation (13) calculates the cumulative start-up costs for a given schedule of generators. The simple heuristic logic outlined in Figure 4 changes the schedule of generators if the additional relative cost from using an alternative generator combination is less than the avoided cumulative start-up cost.

$$F(B) = \sum_{k=1}^N \sum_{i=1}^G c_i \cdot (B_{i,k} > 0 \ \& \ B_{i,k-1} == 0) \quad (13)$$

First, the shortest segment of operation or non-operation is determined. If a generator is scheduled off for a short period, but it would be feasible to keep it on, then the sum of the relative costs is compared to the cost of shutting down and starting up again. If a generator is on for a short period and at each step it is on there is a feasible subset that does not include this generator, then the alternative is considered. If the sum of the additional relative costs is less than the equipment start-up cost, then modify the binary on/off schedule accordingly. Otherwise, the next shortest segment is evaluated.

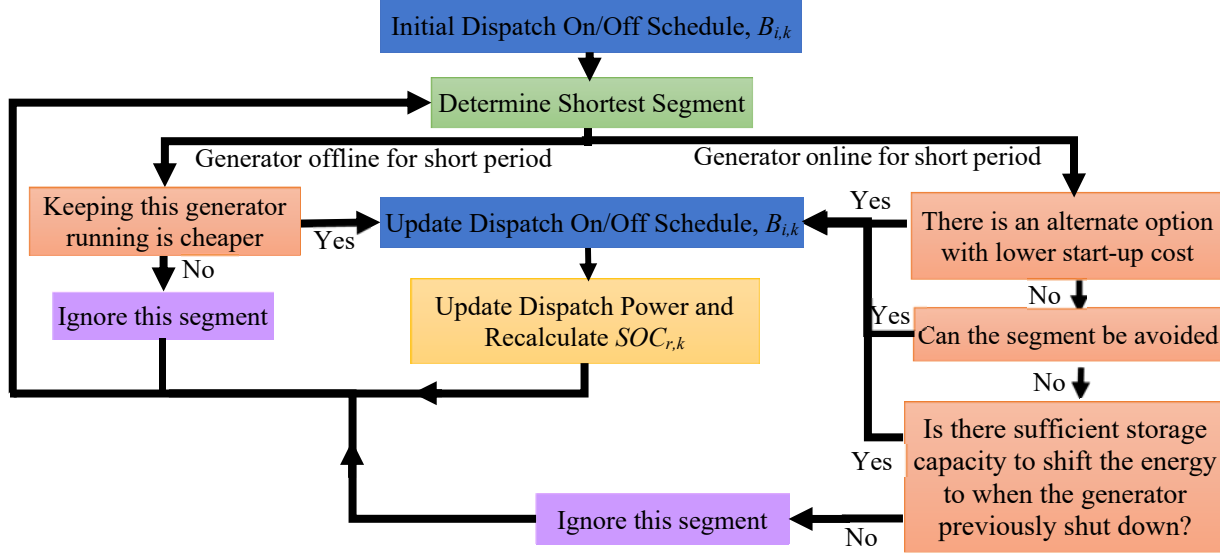


Figure 4 Heuristic method for avoiding costly re-starts

Solving the optimization problem with FMI

The cQP method avoids the binary states of a full mixed integer problem. Equation (14) formulates the problem as a full mixed integer optimization using the binary variables, $B_{i,k}$, and the constraint function (12). The full mixed integer approach solves a single optimization using the coefficients of **Fit B**.

$$\min C = F(B) + \sum_{k=1}^N \left\{ \sum_{i=1}^G F(P_{i,k}) + \sum_{i=1}^G a_0 \cdot B_{i,k} + F(P_{grid,k}) \right\} + \sum_r^S \{F(SOC_r)\} \quad (14)$$

The cQP and mcQP approaches perfectly replicates the full mixed integer solution for many simple arrangements of generators and storage devices. Complex arrangements, such as the 16 component system presented herein, typically yield different outcomes for each of the three approaches. The cQP and mcQP approaches solve the problem more efficiently and more consistently than a commercial mixed-integer solver, Gurobi®.

III. RESULTS

The campus energy system described in Table 1, through Table 4 has 18 components, 15 of which require setpoints and 11 of which require unit commitment. The system accommodates the electric, heat, and cooling demands of a large research university campus. This system tests the differences between the three optimization approaches: the full-mixed integer (FMI) method, the complementary Quadratic Programming (cQP) method, and the modified complementary Quadratic Programming (mcQP) method. Time-of-use electric rates are described in Figure 5. The natural gas cost is \$7.5 per mmBTU and the Diesel fuel cost is \$24 per mmBTU, which is roughly \$3.30 per gallon.

Table 1: Generator component parameters used in the test campus system. The linear and quadratic cost coefficients of Fit B, $[a_0, a_1, \dots, a_j]$ and $[b_1, \dots, b_j]$, are listed along with the linear CHP coefficients, $\beta_0, \beta_1, \dots, \beta_j$. The constant terms, a_0 and β_0 , are used to determine the total operating cost and total heat production

Component	P_i^{min} (kW _E)	P_i^{max} (kW _E)	r_i^{max} (kW _E /hr)	a_0 (\$)	a_1, \dots, a_j (\$/kW)	b_1, \dots, b_j (\$/kW ²)	β_0 (kW _H)	β_1, \dots, β_j (kW _H /kW _E)
Fuel Cell 1 (CHP)	500	2,000	500	16.58	0.0359, 0.0359, 0.0394, 0.0394, 0.0470	0, 3.12e-6, 0, 2.14e-9, 2.27e-5	305.7	0.726, 0.694, 0.645, 0.578, 0.5782
Fuel Cell 2 (CHP)	500	2,000	600	41.54	0.0211, 0.0211, 0.0211, 0.0346, 0.0606	0, 0, 1.35e-5, 9.83e-10, 4.54e-8	752.9	0.494, 0.380, 0.348, 0.348, 0.348
Gas Turbine 1 (CHP)	4,000	7,000	4,000	173.52	0.0653, 0.0653, 0.0653, 0.0700, 0.0717	0, 0, 0, 1.0557e-5, 9.4938e-6	4,257.8	1.033, 1.004, 0.795, 0.795, 0.795
Gas Turbine 2 (CHP)	2,000	5,000	2,000	225.38	0.0416, 0.0416, 0.0688, 0.0688, 0.1270	0, 2.312e-8, 0, 3.071e-5, 0	4,351.2	0.834, 0.778, 0.778, 0.778, 0.778
Gas Turbine 3	100	500	300	21.65	0.0449, 0.0449, 0.0449, 0.0747, 0.1150	0, 0, 1.763e-5, 0, 1.017e-4		
Diesel Generator	500	1,500	1,000	21.81	0.275, 0.275, 0.275, 0.289, 0.292	0, 0, 3.92e-8, 5.88e-7, 5.92e-5		
Heater	2,000	20,000	10,000		0.853, 0.02556	0		
Rooftop PV	0	3,000	∞					

Table 2 Chiller component parameters used in the test campus system. Chiller costs are incurred as the electrical power used by each chiller, determined by the linear energy conversion factors β .

Component	P_i^{min} (kW _C)	P_i^{max} (kW _C)	r_i^{max} (kW _C /hr)	β_0 (kW _E)	β_1, \dots, β_j (kW _E / kW _C)
Chiller 1	2,000	10,000	3,000	183.1	0.133, 0.161, 0.304
Chiller 2	1,500	10,000	2,000	186.1	0.135, 0.157, 0.305
Chiller 3	2,500	7,500	5,000	199.6	0.150, 0.151, 1.52, 0.238, 0.368
Chiller 4	2,000	7,500	2,000	182.9	0.166, 0.222, 0.390

Table 3 Energy storage components used in the test campus system. Energy storage costs are incurred as the power used to charge the device, so there is no direct costs for energy storage.

Component	SOC_i^{max} (MWhr)	P_i^{min} (kW)	P_i^{max} (kW)	κ^* (%/hr), κ (kW)	η_c, η_d (%)
Battery	25.5	-14,900	7,540	0.0, 3.41	99.48, 99.48
Cold Storage	20	-50,000	50,000	0.0, 123.75	99, 99
Hot Storage	7.5	-30,000	30,000	0.0, 330	99, 99

Table 4 Startup costs for fuel cells, gas turbines, diesel generator, and chillers.

Fuel Cell 1	Fuel Cell 2	Gas Turbine 1	Gas Turbine 2	Gas Turbine 3	Diesel Generator	Chiller 1	Chiller 2	Chiller 3	Chiller 4
\$300	\$250	\$1000	\$300	\$10	\$100	\$150	\$200	\$50	\$50

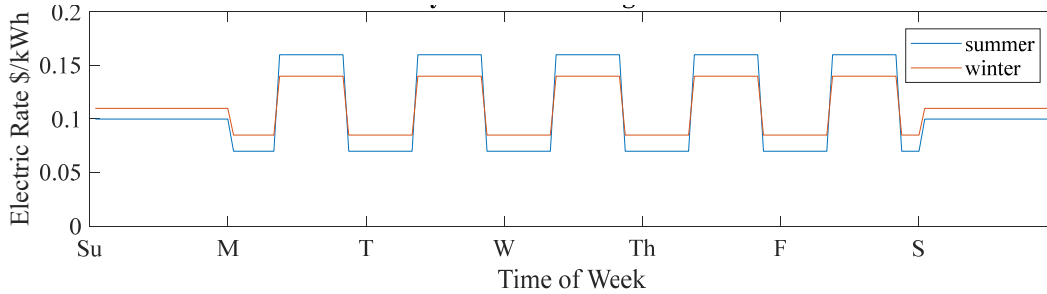


Figure 5 Electric utility rates vary throughout the week and are dependent on season. From June 1st through September 30th summer rates are used, while from October 1st through May 31st winter rates apply. Peak pricing is during the middle of the day on weekdays

Full year energy profiles for electric, heating, and cooling demands collected at a college campus in California are used for the loads, resulting in 8760 optimizations from both cQP and mcQP methods. This allows for comparison of computational time, dispatches, and cost at all ranges in time of day, weekly, and seasonal profiles. The cQP is able to optimize a 24 hour dispatch in an average of 1.6 seconds, while the mcQP method takes on average 6.8 seconds. Both approaches simulated an entire year in a receding horizon control approach where the forecasted loads perfectly matched the actual loads.

Figure 6 compares the distribution of operating costs for each optimization of the 24-hour horizon. The mean cost for the cQP method is \$28,096 with a standard deviation of \$3,870. The mean cost for mcQP method is \$26,992 with a standard deviation of \$3,464. The cQP dispatch averages \$1,104 more expensive than the mcQP dispatch. The lower cost solutions of the mcQP method result from searching a greater space during the unit commitment step. The smaller standard deviation for the mcQP method also indicates a more stable solution for the receding horizon control.

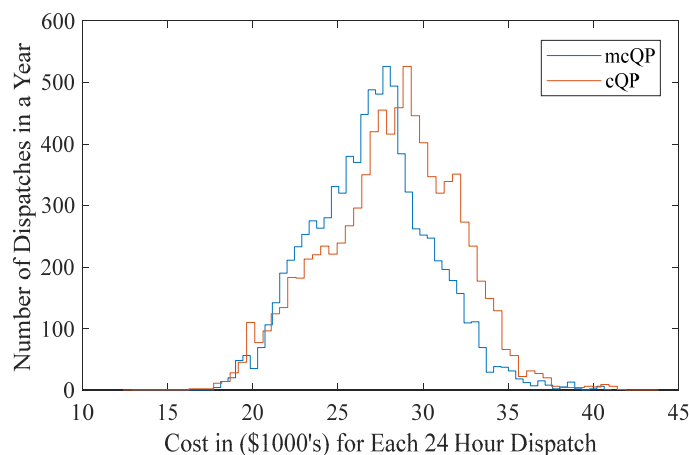


Figure 6 Distribution of operating costs for each optimization of the 24-hour horizon using either the mcQP or cQP methods in a receding horizon control strategy with perfect foreknowledge of the demands.

The full mixed integer problem typically takes longer than an hour to reach a solution. In a receding horizon with hourly timesteps, new component setpoints must be generated in less than an hour, so a time limit was implemented for the full mixed integer approach. The best solution that was found within 3600 seconds of computation was returned. Since the FMI method operates in nearly real time, two weeks were simulated: a winter week from January 8th to 15th, and a summer week from June 25th to July 1st. To facilitate direct comparison of FMI, cQP and mcQP, the initial condition from the previous mcQP optimization was used for all three approaches at each step.

During the winter week the FMI method converged to an optimal solution in less than an hour for 104 of the 168 optimizations, found a non-optimal but feasible solution 10 times, and failed to find a feasible operating condition 54 times. The commercial FMI solver takes longer to find a solution when there is high cooling demand, e.g. summertime, because the multi-unit chiller dispatch further complicates the mixed integer search space. During the summer week the FMI method converged to an optimal solution only 35 times, found a feasible outcome for 17 additional cases, and failed to find a feasible dispatch for 116 of the 168 optimizations. Highly complex scenarios are computationally costly, and a converged or even feasible solution may not be found. Figure 7 compares the distribution of operating costs for each optimization of the 24-hour horizon.

There are fewer cost samples for the FMI method because cost can only be calculated for the feasible scenarios. During the summer week the average 24-hour dispatch horizon cost is \$31,641, \$32,026, and \$31,979 for mcQP, cQP, and FMI respectively. During the winter week simulation the costs are \$26,938, \$27,464, and \$27,339 for mcQP, cQP, and FMI respectively. The mcQP method never fails to find a feasible solution and consistently finds the lowest cost solution in both seasons.

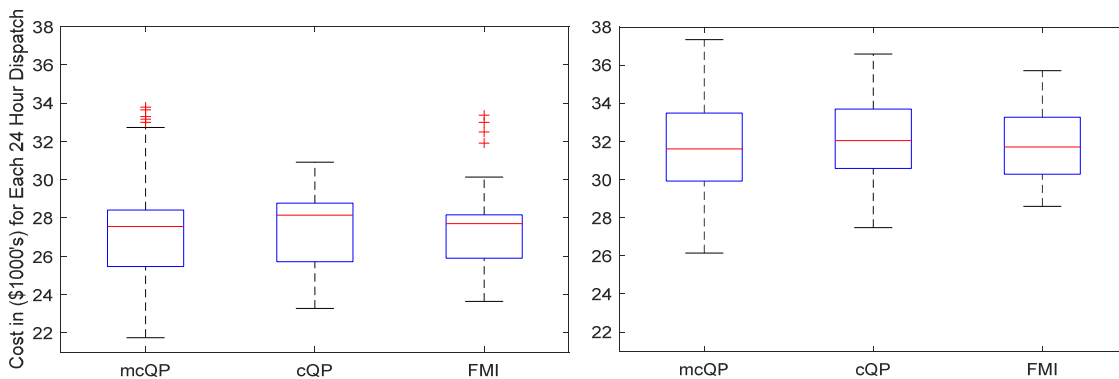


Figure 7 Distribution of operating costs for each optimization of the 24-hour horizon for winter (left) and summer (right). Identical initial conditions are used for solving the mcQP, cQP, and FMI methods

Table 5 Summary of Winter and Summer comparison of FMI, cQP and mcQP optimization methods

Method	FMI	cQP	mcQP
Winter mean cost	\$27,339	\$27,464	\$26,938
Winter std. dev.	\$1,682	\$2,739	\$1,972
Summer mean cost	\$31,979	\$32,026	\$31,641
Summer std. dev.	\$1,983	\$2,588	\$2,160

Figure 8 presents results of a single optimization, midnight of January 8th, for all three methods. For this case, the FMI solver converged on an optimal solution. The figure illustrates only the electric portion of the dispatch solution, as the heating and chilling dispatches showed greater similarity. The hourly cost over the course of a day varies with dispatch and unit commitment. The spikes seen in the cost dispatch are a result of start-up costs as new generators are brought online. The stacked bar chart illustrates the cumulative generation from each component. Tracing the top of the stacked bars, and subtracting the charging power of the storage that appears below the x-axis, equals the net demand at each hour. Discharging storage power is stacked on top of the generation as it adds to the cumulative power. The overlaid line represents the state-of-charge of the energy storage at each timestep. The generation scale is shown on the left while the state of charge scale is shown on the right. The operating costs for each optimization of the 24-hour horizon using identical initial conditions is \$28,442, \$33,648, and \$28,018 for mcQP, cQP, and FMI respectively.

The mcQP method charges the battery in the morning when electric prices are low, and thus operates without the second gas turbine for much of the day. The FMI and cQP solutions avoid using the electric utility altogether. The cQP solution employs the small micro-turbine and diesel recip to make-up additional power, which accounts for the majority of the additional cost. Additional control logic bespoke to this system could improve the general cQP approach by forcing a check of the microturbine and diesel generator operating status. Generally the cQP approach more closely approximates mcQP, and this particular optimization may be one of the outliers of Figure 7.

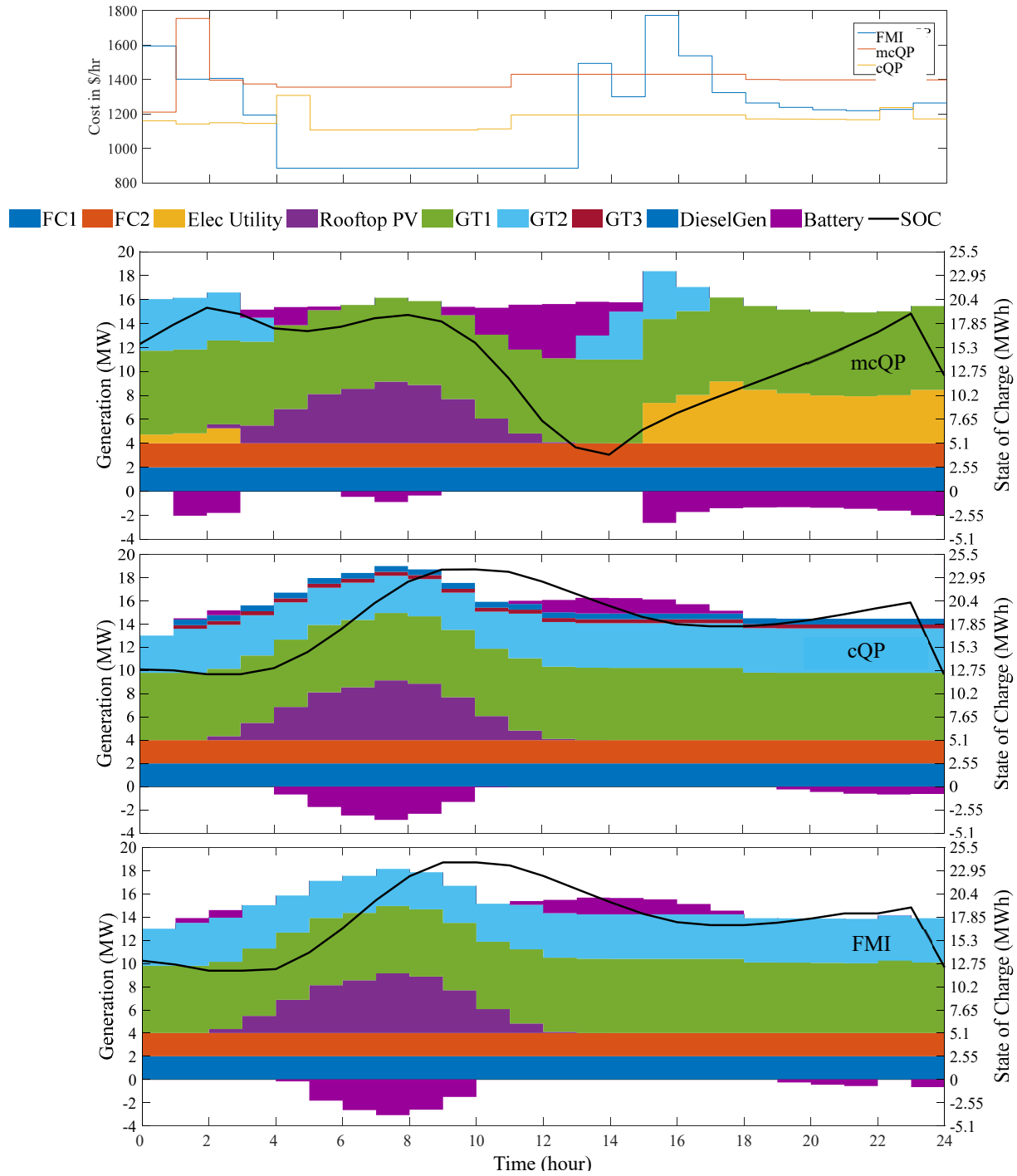


Figure 8 Comparison of electrical dispatch of January 8th for mcQP (top), cQP (middle), and FMI (bottom) methods with the same initial conditions and constrained to have the same ending state of charge. The cost for the FMI method is lowest, followed by mcQP, and cQP

Figure 9 presents results of a single optimization, midnight of June 26th, for all three methods. The operating costs for each optimization of the 24-hour horizon using identical initial conditions is \$34,693, \$35,751, and \$35,141 for

mcQP, cQP, and FMI respectively. The costs and dispatches produced by all three approaches are similar. This particular summer optimization is simpler than most, as evidenced by the FMI method's ability to reach a feasible solution. Unlike mcQP, the cQP method keeps the second gas turbine off from 7-8am, 10am-1pm, and from 6-7pm. During the middle of the day, the cQP method brings GT3 online and relies on the battery and electric utility to compensate for not using GT2. This significantly changes the battery discharge dynamics. The cQP method also reduces the time that the first gas turbine is online. The reduction in use of the larger two gas turbines results in a higher overall cost for cQP, as the utility is more heavily relied on.

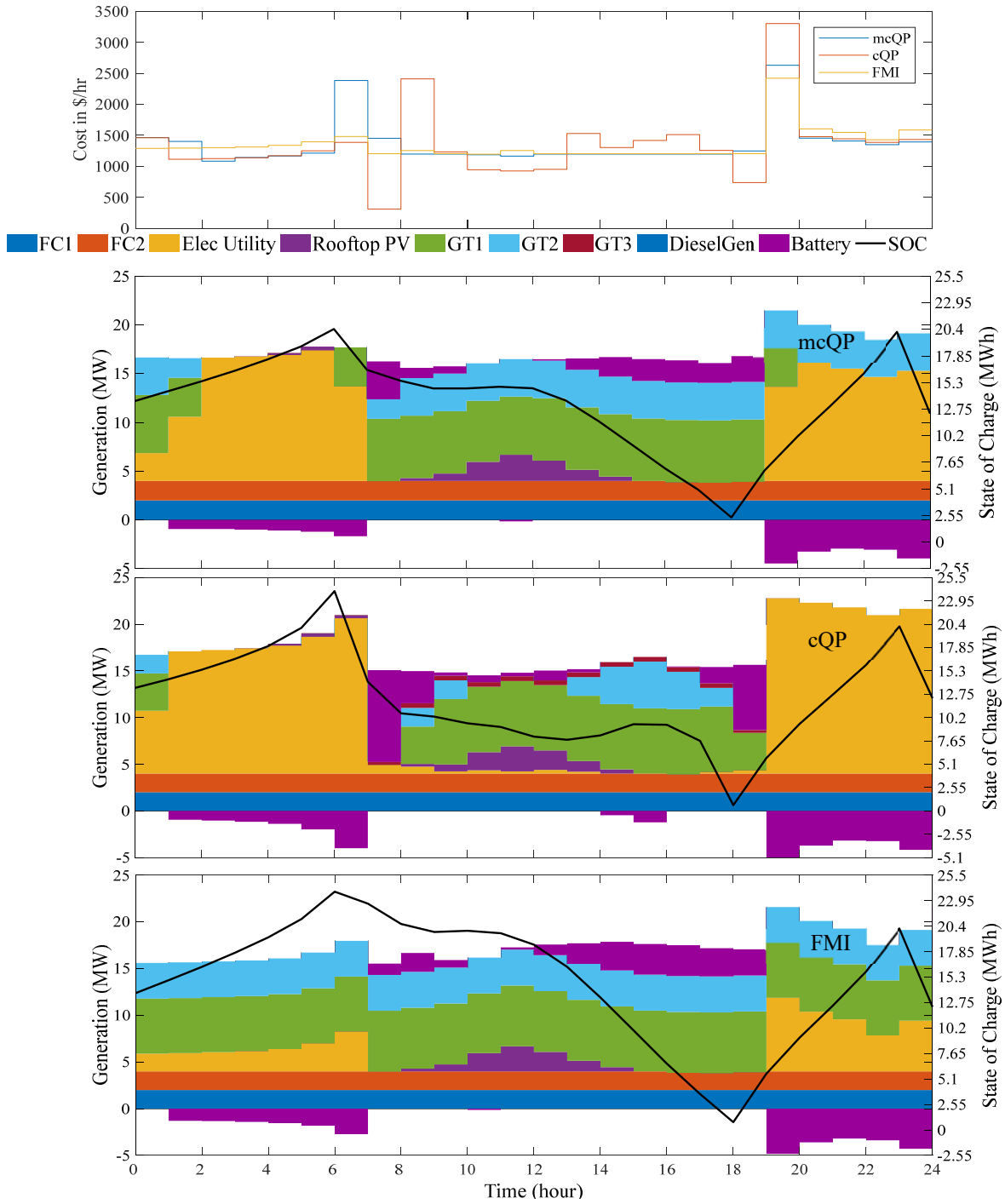


Figure 9 Dispatch from mcQP (top), cQP (middle), and FMI (bottom) methods for June 26th. The cost at each hour for each method is shown at the top.

IV. Conclusion

This paper presented an economic dispatch method which reduces the computational effort of unit commitment applicable to dispatchable energy systems with energy storage. The approach addresses three critical complexities of modern micro-grids: the on/off discontinuity of each generator, the non-linear cost function of each generator, and the simultaneous dispatch required to incorporate energy storage or combined cooling heating and power applications. Energy storage and co-production of heat is incorporated through constraints rather than arbitrary cost terms. Charging and discharging losses are incorporated in such a manner that the dispatch schedule need not be known a priori. Important constraints such as lower and upper operating limits, ramp rate, and storage capacity are also incorporated. The methodology allows energy storage to simultaneously perform energy arbitrage, ramping support and peak shaving. The results illustrated simultaneous optimization of multiple energy products, (e.g. electric, heating, cooling, steam), and captured the natural interdependency of heating/cooling systems with the electric generation. Results indicated that even for complex systems of generators and storage devices, the complete mixed-integer problem can be significantly simplified. Further development will continue on the open-source energy simulation platform: EAGERS.

Acknowledgments

The authors gratefully acknowledge and recognize the funding support from the US-Italy Fulbright Commission and the European Union RESILIENT project.

V. REFERENCES

- [1] A.G. Tsikalakis and N.D. Hatziargyriou, "Centralized control for optimizing microgrids operation," in Power and Energy Society General Meeting, 2011 IEEE, San Diego, CA, 2011, pp. 1-8.
- [2] W. Gu, Z. Wu, R. Bo, W. Liu, G. Zhou, W. Chen, Z. Wu, "Modeling, planning and optimal energy management of combined cooling, heating and power microgrid: A review," *Electrical Power and Energy Systems*, vol. 54, pp. 26–37, 2014.
- [3] A.L. Dimeas and N.D. Hatziargyriou, "Operation of a Multiagent System for Microgrid Control," *IEEE Transactions on Power Systems*, vol. 20, no. 3, pp. 1447 - 1455, 2005.
- [4] S.D.J. McArthur, E.M. Davidson, V.M. Catterson, A.L. Dimeas, N.D. Hatziargyriou, F. Ponci, T. Funabashi, "Multi-Agent Systems for Power Engineering Applications—Part I: Concepts, Approaches, and Technical Challenges," *IEEE Transactions on Power Systems*, vol. 22, no. 4, pp. 1743 - 1752, 2007.
- [5] C. P. Nguyen and A. J. Flueck, "A Novel Agent-Based Distributed Power Flow Solver for Smart Grids," *IEEE Transactions on Smart Grids*, vol. 6, no. 3, pp. 1261-1270, May 2015.
- [6] E. Planas, A. Gil-de-Muro, J. Andreu, I. Kortabarria, and I. Martínez de Alegría, "General aspects, hierarchical controls and droop methods

in microgrids: A review," *Renewable and Sustainable Energy Reviews*, vol. 17, pp. 147–159, January 2013.

- [7] I. Rossi, L. Banta, A. Cuneo, M.L. Ferrari, A.N. Traverso, A. Traverso "Real-time management solutions for a smart polygeneration microgrid", *Energy Conversion and Management*, Vol. 112, pp. 11-20.
- [8] D. McLarty, C. C. Sabate, J. Brouwer, and F. Jabbari, "Micro-grid energy dispatch optimization and predictive control algorithms; A UC Irvine case study," *Electrical Power and Energy Systems*, vol. 65, pp. 179-190, 2015.
- [9] C. Chen, S. Duan, T. Cai, B. Liu, and G. Hu, "Smart energy management system for optimal microgrid economic operation," *IET Renewable Power Generation*, vol. 5, no. 3, pp. 258–267, 2011.
- [10] M. Nemati, M. Braun, S. Tenbohlen, "Optimization of unit commitment and economic dispatch in microgrids based on genetic algorithm and mixed integer linear programming," *Applied Energy* vol 210, pp. 944-963, 2018.
- [11] Liu Xiaoping, Ding Ming, Han Jianghong, Han Pingping, and Peng Yali, "Dynamic Economic Dispatch for Microgrids Including Battery Energy Storage" 2010 2nd IEEE International Symposium on Power Electronics for Distributed Generation Systems pp 914-917, 2010.
- [12] H. Zhang, D. Yue, X. Xie, S. Hu, S. Weng, Multi-elite guide hybrid differential evolution with simulated annealing technique for dynamic economic emission dispatch" *Applied Soft Computing* vol 34 pp. 312-323, 2015
- [13] C. C. A. Rajan, "A solution to the economic dispatch using EP based SA algorithm on large scale power system," *International Journal of Electrical Power & Energy Systems*, vol. 32, no. 6, pp. 583–591, July 2010.
- [14] C.A. Roa-Sepulveda and B.J. Pavez-Lazo, "A solution to the optimal power flow using simulated annealing," *International Journal of Electrical Power & Energy Systems*, vol. 25, no. 1, pp. 47–57, January 2003.
- [15] L. Han, C. E. Romero, and Z. Yao, "Economic dispatch optimization algorithm based on particle diffusion," *Energy Conversion and Management*, vol 105, pp. 1251-1260, 2015.
- [16] A. A. Moghaddam, A. Seifi, T. Niknam, and M. Reza A. Pahlavani, "Multi-objective operation management of a renewable MG (micro-grid) with back-up micro-turbine/fuel cell/battery hybrid power source," *Energy*, vol. 36, pp. 6490-6507, 2011.
- [17] M. Basu, "Artificial immune system for combined heat and power economic dispatch," *International Journal of Electrical Power & Energy Systems*, vol. 43, no. 1, pp. 1-5, December 2012.
- [18] S. Hemamalini and S. P. Simon, "Dynamic economic dispatch using artificial immune system for units with valve-point effect," *International Journal of Electrical Power & Energy Systems*, vol. 33, no. 4, pp. 868-874, May 2011.
- [19] S. Pothiya, I. Ngamroo, and W. Kongprawechnon, "Ant colony optimisation for economic dispatch problem with non-smooth cost functions," *International Journal of Electrical Power & Energy Systems*, vol. 32, no. 5, pp. 478–487, June 2010.
- [20] Y.H. Song, C.S. Chou, and T.J. Stonham, "Combined heat and power economic dispatch by improved ant colony search algorithm," *Electric Power Systems Research*, vol. 52, no. 2, pp. 115–121, 1999.
- [21] M. Motevasel, A. Reza Seifi, and T. Niknam, "Multi-objective energy management of CHP (combined heat and power)-based micro-grid," *Energy*, vol. 51, p. 123e136, 2013.
- [22] T. Niknam, R. Azizipanah-Abarghooee, A. Roosta, and B. Amiri, "A new multi-objective reserve constrained combined heat and power dynamic economic emission dispatch," *Energy*, vol. 42, pp. 530-545, 2012.
- [23] A. J. del Real, A. Arce, and C. Bordons, "Combined environmental and economic dispatch of smart grids using distributed model predictive control," *Electrical Power and Energy Systems*, vol. 54, pp. 65–76, 2014.

- [24] K. A. Pruitt, R. J. Braun, and A. M. Newman, "Evaluating shortfalls in mixed-integer programming approaches for the optimal design and dispatch of distributed generation systems," *Applied Energy*, vol. 102, pp. 386–398, 2013.

V. APPENDIX

Appendix I, Determining the value of stored energy at the end of the dispatch horizon:

Giving value, e.g. negative cost, to the *SOC* at step N , ensures that the optimal solution does not fully deplete the stored energy reserves. The function describing the value of this residual charge, (15), is a convex quadratic such that the first kWh of storage is valued slightly more, $I+\delta$, than the highest marginal cost dispatchable generation, and the last kWh of storage is valued less than, $I/(I+\delta)$, the smallest marginal cost of generation. The discharge efficiency, η_d , is included because only the energy that can be extracted has value.

$$\{F(SOC_r)\}_N = a_1 \cdot (SOC_r)_N + \frac{1}{2} a_2 \cdot (SOC_r)_N^2 \quad (15)$$

$$a_1 = -\eta_d \cdot (1 + \delta) \cdot \max_i \left(\frac{dF(P_i)}{dP} \right) \quad (16)$$

$$a_2 = \eta_d^2 \cdot \left\{ (1 + \delta) \cdot \max_i \left(\frac{dF(P_i)}{dP} \right) - \frac{1}{(1 + \delta)} \cdot \min_i \left(\frac{dF(P_i)}{dP} \right) \right\} / P_i^{max} \quad (17)$$

The steep negative slope, a_1 , at zero *SOC* implies a preference to use the most expensive generator before fully depleting the storage. Similarly, the less negative, or possibly positive, slope at full *SOC*, $a_1 + a_2$, suggests a preference to discharge storage before using the least expensive dispatchable generator. This method does not assign cost or value to stored energy at intermediate time steps, thus ensuring maximizing utilization within the dispatch horizon.

Appendix II, Energy storage boundary constraints:

Over charging or over discharging energy storage may damage or reduce the life of the system. When energy storage is relied upon to provide the moment-to-moment balancing of generation and demand soft boundary constraints encourage a buffer when the storage is nearly completely charged or discharged. A simple approach optimizes the middle 80% of the available capacity, leaving 10% as a buffer for uncertainty. This approach underutilizes the storage device. Alternatively, boundary constraints implemented through the cost function allow dispatching the capacity between 90% and 100% SOC when utilizing that capacity provides significant additional value. A quadratic cost penalty in the modified cost function, equation (18), is constrained by (19). The value of a boundary state, u , is zero when the storage is at or below 90% SOC, and grows as the storage approaches 100%. As

the SOC approaches 0% a second boundary state, l , and corresponding constraint, equation (20), applies. The buffer can be proportional, Π , to the maximum capacity of the storage, or a fixed value. The severity of the quadratic penalty determines the relative ‘softness’ of the boundary and can be in addition to the hard capacity constraint (7).

$$\min C = \sum_{k=1}^N \left\{ \sum_{i=1}^G F(P_i)_k + F(P_{grid})_k + \sum_r^S F(l_k + u_k) \right\} + \sum_r^S \{F(SOC_r)\}_N \quad (18)$$

$$\Pi \cdot SOC_r^{max} \geq (SOC_r)_k - u_k \quad \& \quad u_k \geq 0 \quad (19)$$

$$\Pi \cdot SOC_r^{max} \geq -(SOC_r)_k - l_k \quad \& \quad l_k \geq 0 \quad (20)$$

Appendix III, Least squares problem formulation for determining the piecewise cost coefficients:

The data used to calibrate the individual generator cost functions, i.e. $F(P_i)$ for generator i at power P_i , consists of individual data points, d , for power output, $(P_i)_d$, and fuel input, Y_d . The objective of the least squares problem, equation (21), is to find the curve fitting coefficients, a_j and b_j , that minimize the sum of errors between the fit cost and the recorded data in set D . The piecewise quadratic cost function is described by equations (22) and (23). The piecewise quadratic has been generalized to m segments, S_j , each with a corresponding length, S_{max_j} . The output, $(P_i)_d$, is divided into these segments in order, such that $S_1 = S_{max_1}$ before S_2 has a value greater than zero.

$$\min_{a_j, b_j} C = \sum_{d=1}^D \{F(P_i)_d - Y_d\}^2 \quad (21)$$

$$F(P_i)_d = \sum_{j=1}^m \{a_j \cdot S_{j,d} + b_j \cdot S_{j,d}^2\} \quad (22)$$

$$\forall d \quad (P_i)_d = \sum_{j=1}^m S_{j,d} \quad s.t. \quad \forall j \quad S_{j,d} \leq S_{max_j} \quad (23)$$

Constraint equation (24) ensures a convex fit, while constraint equation (25) ensures a tight fit at maximum output, i.e. $Fit_{max} = Y_{max}$, where Y_{max} corresponds to the cost at $max(X_d)$.

$$\forall j > 1: \quad a_{j-1} + b_{j-1} \cdot S_{max_j} - a_j \leq 0 \quad (24)$$

$$Y_{max} = [a_1 \quad \dots \quad a_j \quad b_1 \quad \dots \quad b_j] \bullet [S_{max_1} \quad \dots \quad S_{max_j} \quad S_{max_1}^2 \quad \dots \quad S_{max_j}^2] \quad (25)$$

With some straightforward conversion the least-squares problem can be formulated into the a quadratic programming formulation, $\min C = x'Hx + f'x$. The open-source interior point method used in EAGERS can then solve for the **Fit A** coefficients. Since most generators do not perform at their highest efficiency at low power, the first segments of **Fit A** will generally be linear, i.e. $b_l = 0$. A simple uniqueness check on the linear cost coefficients of the

first segment, a_l , will ensure that typically only a single generator is dispatched within the relaxed constraint region. At times, the ramping constraints may force two or more generators to operate in the first linear segment, but this does not cause an issue with the proposed cQP method.

The addition of a constant term, a_0 , to equation (22), results in equation (26). Substituting this equation solves for **Fit B** coefficients.

$$F(P_i)_d = a_0 + \sum_{j=1}^m \{a_j \cdot S_{j,d} + b_j \cdot S_{j,d}^2\} \quad (26)$$

A separate optimization can determine the optimal segment lengths. Many generators have peak operational efficiencies at or near rated capacity, in which case a linear approximation is equivalent to **Fit A**. However, chillers, fuel cells and other distributed energy systems operate more efficiently at part load. In these instances a piecewise quadratic cost drives the solution towards these optimal operating conditions, where a linear fit would not. **Fit B** provides a significant improvement in the accuracy of the fit, particularly at part load. The coefficients, a_j and b_j , are arranged into a sparse quadratic programming formulation. Equation (27) illustrates the sub-block of the quadratic programming formulation associated with generator i at step k . The convex nature of the fit will ensure $S_j = S_j^{max}$ before $S_{j+1} > 0$.

$$C_{i,k} = [S_1 \quad \dots \quad S_j]_k \cdot \begin{bmatrix} b_1 & 0 & 0 \\ 0 & \ddots & 0 \\ 0 & 0 & b_j \end{bmatrix} \cdot \begin{bmatrix} S_1 \\ \vdots \\ S_j \end{bmatrix}_k + [a_1 \quad \dots \quad a_j] \cdot \begin{bmatrix} S_1 \\ \vdots \\ S_j \end{bmatrix}_k \quad (27)$$

Appendix IV, Segmented linear fits for CHP and Chillers

Combined heating and power generators, CHP, produce output appearing in two energy balances for a single input feedstock. The secondary heating output model must be linear to be enforced through the energy balance constraints, i.e. heat output = $P_i \cdot \beta$ or $sum(S_j \cdot \beta_j)$. The linear coefficients, β_j , must decline to maintain convexity, meaning that the marginal heat production must be less as power output increases. This trend is common in most combustion based CHP, but not all fuel cell generators. A constant amount of heat production, β_0 , when the generator is known to be on is included in **Fit B** to improve the estimate of heat recovery.

Electric chillers typically represent a non-linear conversion of electrical power to cooling power not captured by a constant coefficient of performance. Without cold thermal storage, there is little flexibility in meeting the thermal demand, and chillers are often run at non-optimal performance. In this scenario, it is preferable to first optimize the

chiller dispatch independent of other systems, where the linear and quadratic cost terms represents the non-linear electric power consumption. An optimization of the chilling system is done first, then the resulting electric consumption of the chillers is added to the net electric load. A second optimization sequence then proceeds for the remaining energy systems.

With cold energy storage, it becomes feasible to use chiller loads to balance the electric demand, and thus dispatch all systems concurrently. In this scenario, the chillers have no direct costs, i.e. $F(P_i) = 0$. They appear in the electric energy balance as a load, $-P_i \cdot \beta$ or $sum(-S_j \cdot \beta_j)$, and in the cooling energy balance as a generator, P_i . Given the flexibility in dispatch afforded by the thermal storage, it is generally preferable to operate all chillers at their design condition, thus justifying the assumption of a linear model.

Appendix V. Converting energy storage to a dispatchable generator:

The global horizon perspective is incorporated at each step by using the *SOC* determined by the first optimization to set the nominal discharge target, P_r^0 . A quadratic cost constrains deviations from the original storage forecast, but allows for deviations when significant savings can accrue. The energy balance at each step thus becomes (28). The planned power output from the storage is placed on the right-hand-side as a constant. The deviation from this power, and the charging penalty remain on the left hand side.

$$\sum_{i=1}^G P_i + P_{grid} + \sum_{r=1}^S (P_r^* - \phi_r) = L - P_r^0 \quad (28)$$

The planned power output, P_r^0 , can be calculated based on the *SOC* states from the first optimization, (29), including any proportional or fixed losses, κ^* or κ . The allowable range of the deviation is thus the nominal power output range of the storage device shifted by P_r^0 as per (30). The power output might be further constrained by the available stored energy or remaining storage capacity if that is more restrictive given the current *SOC*.

$$P_r^0 = - \frac{\{(SOC_r)_k - (1 - \kappa^* \cdot \Delta t_k) \cdot (SOC_r)_{k-1} - \kappa\} \cdot \eta_d}{\Delta t_k} \quad (29)$$

$$P_r^{min} - P_r^0 \leq P_r^* \leq P_r^{max} - P_r^0 \quad (30)$$

The charging penalty must similarly be offset by the planned power output, as per (31).

$$\phi_r \geq \left(\frac{1}{\eta_c} - \eta_d \right) \cdot \left[\frac{-P_r^0}{\eta_d} - P_r^* \right] \quad (31)$$

After testing all feasible options at each step, the lowest cost option is selected and the *SOC* profile updated using (32) and solving equation (9) for $(SOC_r)_k$. Equation (32) combines the initial energy storage dispatch with the storage deviation from the lowest cost option.

$$(P_r)_k = P_r^0 + P_r^* \quad (32)$$